Available online at www.sciencedirect.com
ScienceDirect
Earth and Planetary Science Letters 259 (2007) 372–383
EPSL
www.elsevier.com/locate/epsl

Colloid diffusion in crystalline rock: An experimental methodology to measure diffusion coefficients and evaluate colloid size dependence

Ursula Alonso [a,*], Tiziana Missana [a], Alessandro Patelli [b], Valentino Rigato [c], Jacopo Ravagnan [c]

[a] CIEMAT, Avda. Complutense 22, 28040 Madrid, Spain
[b] CIVEN, Via delle Industrie 9, 30175 Venezia-Marghera, Italy
[c] LNL-INFN, Viale dell'Universitá 2, Legnaro, Padova, Italy

Received 7 February 2007; received in revised form 25 April 2007; accepted 27 April 2007
Available online 8 May 2007
Editor: R.W. Carlson

Abstract

Colloids present high sorption for many solutes and are considered potential contaminant carriers in geological environments. Experimental quantitative data are required for an adequate description of colloid-mediated contaminant transport within natural media. In this study, a methodology applying the nuclear ion beam technique Rutherford Backscattering Spectrometry (RBS) was used to measure colloid diffusion in crystalline rock and to analyze the effects of colloid size. It was found that colloids diffused within granite, colloid diffusion being both size-dependent and size-limited. Smaller colloids showed faster diffusion while diffusion was hindered for larger colloids of 250 nm. The measured apparent diffusion coefficients (D_a) ranged from 7E-18 m^2/s for 2 nm to 1.5E-18 m^2/s for 100 nm colloids. These diffusion coefficients measured for gold colloids in granite are about five orders of magnitude lower than values found for weak or non-sorbing solutes, under the same experimental conditions. The experimental evidence of colloid diffusion in granite is described here for the first time.

Keywords: diffusion; colloids; crystalline rock; RBS; radioactive waste

1. Introduction

Colloids present high sorption capacity for many solutes and are considered potential contaminant carriers in natural media (Kersting et al., 1999; Ryan and Elimelech et al., 1996). Colloid-driven transport has been implicated in the migration of heavy metals and radiotracers and it is a cause of concern in assessing the long-term performance of deep geological repositories (DGR) of radioactive waste, especially those hosted in crystalline rock, currently considered suitable rock formations for a DGR (Missana et al., 2006). Colloids are present in many granitic media (McCarthy and Degueldre, 1993; Degueldre et al., 1996) and can contribute to the radionuclide transport. However, colloid contribution to radionuclide transport in a

* Corresponding author. Tel.: +34 913466183; fax: +34 913466542
E-mail address: ursula.alonso@ciemat.es (U. Alonso).

0012-821X/$ - see front matter © 2007 Elsevier B.V. All rights reserved.
doi:10.1016/j.epsl.2007.04.042

DGR is not always accounted for because of the existing uncertainties and the shortage of experimental quantitative data on colloid migration in geological environments (Alonso et al., 2006).

In fractured rocks, contaminant and colloid transport is assumed to take place by advection in the fracture network favored by the water flow (Grindrod, 1993; James and Chrysikopoulos, 1999; Kosakowsky, 2004; McCarthy and Zachara, 1989; Möri et al., 2003a; Smith and Degueldre, 1993; Oswald and Ibaraki, 2001). Colloid transport largely differs from solute transport because of physical factors including: water velocity, particle size, particle surface charge, particle density or surface area accessible to collisions within the rock surface that can lead to filtration (Hunter, 1986).

Colloid diffusion in a rock matrix can eliminate colloids from the flow paths, but experimental evidence of colloid diffusion remains scarce. The extent of diffusion is expected to be dependant on rock porosity and pore size and therefore size-dependent (Cumbie and McKay, 1999), resulting from exclusion caused by the smaller pore spaces or by the existence of tortuous paths; and after initial colloid diffusion, the particles clog the pores, limiting further diffusion.

Since crystalline rock presents very low porosity (0.2–1%) (Möri et al., 2003b; Kelokaski et al., 2006), colloid diffusion is considered a minor mechanism, but often the concept of matrix diffusion is invoked to interpret the tailing behavior of colloid breakthrough curves in transport experiments (James and Chrysikopoulos, 1999; Kosakowsky, 2004; Möri et al., 2003a). As experimental values are lacking, the diffusion coefficients used to describe the tail of the curve are the parameters which best fit the experimental data but the validity of the parameters obtained is difficult to verify. The experimental determination of colloids diffusion coefficients would be useful to gain a more precise description of colloid transport within crystalline rock.

The aims of this study are: to demonstrate that colloids diffuse within crystalline rock, to estimate their diffusion coefficients and to evaluate colloid size dependence. As no previous experimental work on colloid diffusion within granite existed, primarily because conventional techniques for studying diffusion in low porosity media require long experimental times even for solutes, a novel approach is required.

A methodology applying the nuclear ion beam technique Rutherford Backscattering Spectrometry (RBS) was developed to measure colloid diffusion in crystalline rock and to analyze the effects of colloid size. This technique, widely applied in material science, allows a quantitative in-depth compositional analysis at the micrometer scale (Chu et al., 1978), but is infrequently used for studying geological materials because of their heterogeneity.

In a previous study, this technique was successfully used to study uranium diffusion within granite (Alonso et al., 2003a,b) measuring diffusion coefficients similar to those obtained by "conventional experiments" (Ohlsonn and Neretnieks, 1997). RBS analysis of colloid diffusion on a non-perfectly smooth surface, as granite, needs to be carefully treated. The coexistence of surface roughness, particle retention on the surface and colloid diffusion could lead to a wrong interpretation of the RBS spectra. Therefore, a previous complementary study was carried out to support and to validate the RBS analysis of colloid diffusion on granite and it was published elsewhere (Patelli et al., 2006). In this complementary work it was concluded that it is possible to analyze colloid diffusion within granite by RBS, and that neither granite sample roughness nor particles accumulated on the surface influenced the RBS spectra and further obtained diffusion coefficients for colloids, supporting the validity of the measurements presented here.

2. Materials and methods

2.1. Gold colloids characterization

Commercial gold colloid suspensions obtained from HAuCl4 were used (BBInternational). The negatively charged nanoparticles were produced by gold reduction with the negative charge believed to come from dichlorogold (I) ions adsorbed on the colloids outer surface (Hayat, 1989). As indicated by the supplier, the colloids were suspended in pure water and only containing a residual gold chloride concentration of 0.001%. Gold colloids were selected for their stability, easy identification with RBS in geological materials and their availability in monodisperse size distributions.

The diffusion experiments were performed with Au colloids of 2, 20, 40, 100 and 250 nm to evaluate size dependence. Previous to these diffusion experiments, the size and the stability of all commercial gold colloids were verified by measuring their hydrodynamic diameter with Photon Correlation Spectroscopy (PCS). The PCS measurements performed for all colloid suspensions gave similar values to those indicated by the supplier (Table 1) except the 20 nm Au colloids, which could not be verified with PCS, because they showed strong adsorbance at $\lambda = 514$ nm (the wavelength of the

Table 1
Summary of the main characteristics of the "as-received" gold colloids

Colloids	Particles (ml)	Concentration (ppm)	Conductivity (μS/cm)	Hydrodynamic diameter (nm) (measured by PCS)	Zeta potential (mV)	pH
Au 2 nm	15·E+13	12.1±0.2	8.0±0.2	5.4±0.7	−31.3±0.7	6.19
Au 20 nm	7·E+11	56.8±0.2	8.0±0.2	Not determined (*)	−32.5±1.2	6.06
Au 40 nm	9·E+10	58.2±0.2	8.0±0.2	47.3±0.6	−34.1±1.5	6.16
Au 100 nm	5.6·E+9	56.6±0.2	9.0±0.2	95.0±2.6	−29.8±2.4	5.46
Au 250 nm	3.6·E+8	56.8±0.2	8.0±0.2	221.0±2.4	−59.8±0.5	7.80

(*) High absorbance observed at the wavelength used in PCS.

PCS laser), as confirmed by UV–Vis spectrometry (Alonso et al., 2005).

Stability of the gold colloid suspensions, diluted in deionised water (1:25), was studied evaluating the coagulation kinetic with PCS as a function of the pH. The mean colloid size remained constant during the observation time (1 h) at pH 6 and higher, whereas a significant increase in colloid size was observed at pH 3, indicating coagulation. Under the experimental conditions selected for the diffusion experiments (pH ~6), the gold colloids were stable (Alonso et al., 2005).

A Malvern Zetamaster equipped with a 5 mW He–Ne laser (λ=633 nm) was used to measure the zeta potential (ζ) as a function of the pH in diluted (1:25) suspensions. Gold colloids are negatively charged over almost the whole pH range with an isoelectric point near pH 3, responsible for the rapid coagulation near this pH (Alonso et al., 2004). A summary of the colloids main characteristics: concentration, conductivity, pH, hydrodynamic diameter and zeta potential (ζ) is presented in Table 1. For diffusion studies, the colloid suspensions were used "as-received".

2.2. Granite

The natural granite selected in this study is granodiorite type and comes from "Los Ratones" mine located in the Albalá Granitic Pluton, in the Variscan Iberian Massif (Cáceres, southwest Spain). Its mineral composition consists of quartz (33–35%), plagioclase (29–32%), K-feldspars (26–28%), muscovite (5–6%) and biotite (2–3%). Additionally, it presents corderite, andalucite, ilmenite and zircon (Buil, 2002).

Samples were sectioned with a diamond slab saw to a thickness of approximately 400 μm, mechanically grinded to 30 μm and polished with carborundum to standardize surface roughness, looking for proper interference colors by using a cross-polarized light microscope. Surface roughness of the granite samples was experimentally studied by Atomic Force Microscopy (AFM) in contact-mode. The typical values of statistical parameters including Ra (arithmetical average roughness) and Rz (ten points height) were respectively 0.21 μm and 1.1 μm, on a scale of 6×6 mm^2. The effect of this roughness on the RBS measurements was investigated under our experimental conditions in the above - mentioned complementary study (Patelli et al., 2006).

Typical pore size for this type of granite ranged from 50 to 200 nm, with some fissures in the micrometer range (Alonso et al., 2003b). The diffusion-accessible interconnected porosity of the granite samples was determined with ^{14}C-PMMA impregnation technique and film autoradiography, full details on this technique can be found elsewhere (Hellmuth et al., 1993). In average, this granite presented an accessible porosity of 0.3%.

The main mineral specific porosities were also analyzed: quartz minerals showed no accessible porosity, and feldspars showed porosity coincident with the granite in average (0.3%). Dark minerals that represent about an 8% in volume had higher porosity values (>1.1%) (Leskinen et al., 2007). Significant artifacts on the granite samples caused by the preparation method can be discarded (Hellmuth et al., 1993; Leskinen et al., 2007).

The ζ-potential of the crushed granite and its major minerals was measured in a separate study. Powder granite had, in average, a negative surface charge in the all pH range, with a mean ζ value of approximately −20 mV for pH >4. The major minerals, quartz, plagioclases or feldspars had similar ζ-potential to the granite in average. Only biotite, that represents a 2% in volume of the total granite, presented a positive charge ($\zeta \approx 15$ mV) for pH lower than 6 (Alonso et al., 2004).

The possible attachment of gold colloids to granite surface was evaluated on crushed granite with batch sorption tests using 40 nm colloids (diluted 1:5 in water, granite concentration 1 g/mL, pH 5.7). The distribution coefficient (R_d) was calculated with:

$$R_d = \frac{C_i - C_f}{C_f}\frac{V}{m} \quad (1)$$

C_i and C_f are the initial and final gold concentrations in the solute, V solute volume and m the mass of the rock. The gold concentration, before and after the separation of the rock phase, was determined with UV–Vis spectrometry (λ=527 nm). Low colloid sorption on granite was observed, with R_d of ~1 mL/g.

2.3. Diffusion experiments

Granite slices, previously saturated in low mineralized granitic water (Na-HCO_3 type, pH 8.3 and conductivity 282 μS/cm), were immersed in gold colloid suspensions (Table 1). Six contact times ranging from 5 min to 4 days were selected taking into account the maximum penetration depth that can be investigated by RBS under our experimental conditions (Alonso et al., 2003a).

After contact with the gold colloid suspensions, the granite samples were cleaned with ethanol to minimize the presence of particles accumulated on the surface that could bias the analysis of the diffusion process. The granite surfaces were later analyzed with Rutherford Backscattering Spectrometry (RBS) under the same experimental conditions as previously described herein (Alonso et al., 2003a; Patelli et al., 2006).

RBS spectra were analyzed with the X-RUMP code (Windows version of RUMP) (Doolittle, 1986; http://www.genplot.com/). This computational algorithm simulates the backscattering phenomenon and provides a highly effective tool for interpreting RBS data. Spectrum simulation is performed, in an iterative manner, by defining a theoretical sample substrate, with a specific elemental composition and structure, to achieve an optimum set of parameters allowing a fit of a given spectrum. Impurities and diffusion profiles are simulated by generating fine layers of a varying in-depth composition.

3. Results and discussion

3.1. Application of RBS to diffusion studies in granite

RBS is suitable to determine the concentration of trace elements heavier than the major constituents of the substrate in the samples near-surface region (several μm). A high energy ion beam ($^4He^+$, 2.2 MeV) is directed at the sample with the number of scattered ions and their energy providing with the RBS spectrum. The energy of the backscattered ions basically depends on the incident ion energy and on the mass of the irradiated sample atoms. For elastic collision, the amount of energy transferred to the sample atom and to the backscattered ion depends on the mass ratio of the incident ion and the sample atom. Therefore, the measurement of the backscattered ion energy allows the elemental sample composition to be derived. If the incident ion does not hit the sample atom at the surface, but instead hits a deeper lying atom, the backscattered ion loses energy proportionally to its penetration depth and the samples *stopping power* (Chu et al., 1978). This means RBS can also be used to define a depth profile of the sample composition. Details of the RBS technique can be found elsewhere (Chu et al., 1978).

The application of RBS on granite samples initially presented difficulties because it is a multi-element material spatially heterogeneous. The area analyzed by RBS is approximately 1 mm^2 allowing the characterization of the surface of a single mineral: therefore from an area to another the spectra can vary significantly. However, the RBS spectra from “whiter areas” of the granite specimen corresponding to minerals such as feldspars, quartz or plagioclases, did not show significant variation (Alonso et al., 2003a). Since these three minerals, that represents a 90% of the granite constituents, have the same zeta potential that the whole granite and feldspars had the same porosity than the granite (0.3%) in average, in this study only feldspars areas were analyzed with RBS. As one of the aim of this work was to analyze size-dependant colloid diffusion coefficients, it is important to perform the RBS analyses on areas with comparable spectra.

Fig. 1A shows an example of the RBS spectrum of a granite sample. The channels (energy) corresponding to the main elements of the granite are indicated, as well as their contribution to the spectrum. Elements with high mass produce high yields (intensities in the RBS spectra) and elements of lower mass produce lower yields but all the signals appear superimposed in the spectrum, as shown in Fig. 1A. Fig. 1B shows a magnification of the higher energy region of the granite spectrum. It is clearly seen that, in granite, no signal is detected for energies corresponding to elements heavier than Ba. In the investigation of diffusion profiles in granite it is thus recommended to select heavy elements such as Au.

To obtain an average granite composition, the simulation RBS spectra (plotted as a continuous line) was performed with the RUMP code. It resulted in an elemental composition, given in atomic weight (%), presented in Table 2, together with the composition reported in the literature for the same granite (Buil, 2002). It can be appreciated that the values obtained by RBS are fully comparable with those reported for the granite (Buil, 2002). The relative analytical error of

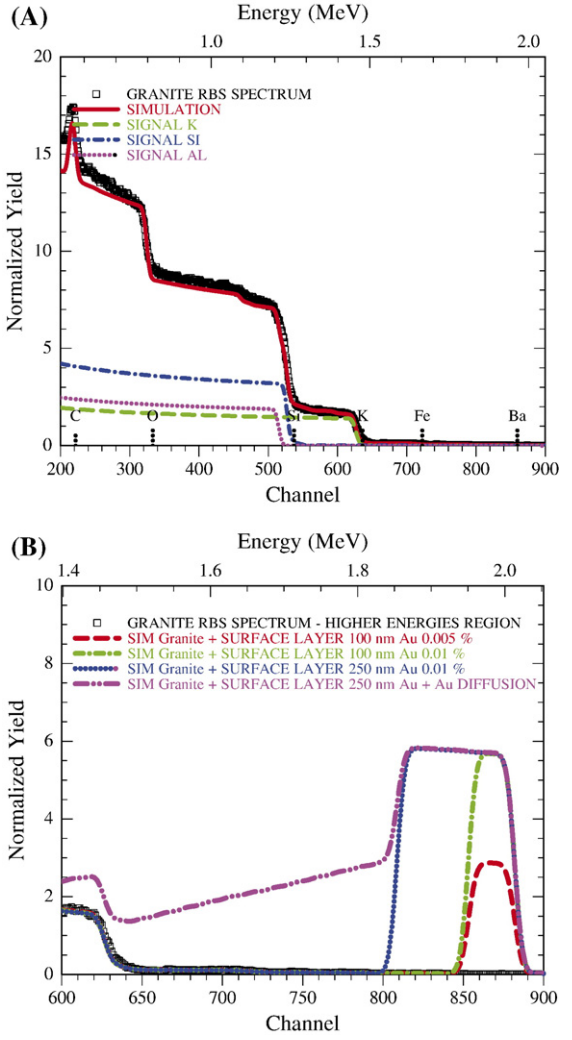

Fig. 1. (A). Experimental RBS spectrum of feldspar with the simulation. The signals from K, Si and Al are plotted. (B) Magnification of the spectrum limited to the higher energy region: the dash (red) line corresponds to the simulation of a 100 nm layer at the granite surface with a Au (0.005 at.%). The (green) dash-dot line corresponds to the simulation of Au surface layer with doubled concentration. The (blue) dot line corresponds to the simulation of 250 nm Au layer at the surface (0.01 at.%). The (magenta) dash dot dot line corresponds Au at the surface and diffused within granite. (For interpretation of the references to colour in this figure legend, the reader is referred to the web version of this article.)

RBS, in determining elemental concentration is below 5%, with a sensitivity of 10^{11}–10^{12} atoms/cm^2 and with a resolution of 100–300 Å at depths of 1 mm.

After the composition of the granite substrate was defined, to simulate that a heavy element was diffusing it was necessary to show that a concentration gradient within this substrate existed. Therefore in the simulation the entire substrate defined for the granite sample was divided into thin sub-layers (with same composition) in which the concentration of the diffusing impurity (Au) was gradually varied.

Possible behaviors of a Au impurity at the granite surface or diffusing within granite are simulated in Fig. 1B. The open-points plot represents the experimental spectrum of granite "substrate"; the dashed line represents the hypothetical simulated RBS spectra of a granite sample peak with a certain Au concentration (0.005% in atomic weight) at a surface sub-layer of 100 nm (limited to the energies of interest for Au). It can be seen that the Au peak (2.1 MeV) is relatively narrow and symmetric. In this example, the Au concentration is lower than the concentration of Fe within the granite substrate (0.02 %), but the Au signal is much more visible than the Fe one. Even having the same concentration, high atomic masses produce a high yield and low atomic numbers (Fe), appearing at lower channels (1.7 MeV) produce a lower yield.

When the gold concentration at the granite surface sub-layer of 100 nm is doubled, the Au peak height increases correspondingly, but the width is constant (Fig. 1B, dash-dot line). The Au peak can be widened by increasing the thickness of the surface sub-layer from 100 to 250 nm (Fig. 1B, dotted line), given the same Au concentration.

If Au is not only located on the surface but also diffuses within the granite, the existence of a sequence of sub-layers, each with different Au concentration, must be considered. The shape of the peak when the Au diffuses in the granite substrate is asymmetrical reflecting lower backscattered energy. The dashed-

Table 2
Comparison of the mean chemical composition (wt.%) of the Spanish granite reported in (Buil, 2002) and obtained simulating the RBS spectra with RUMP

Element	% atomic reported composition	% atomic composition RBS spectrum simulated
O	57.67	60.32
Si	16.00	17.38
Al	16.06	13.29
Na	4.19	3.58
K	3.69	3.89
Ni	1.19	0.03
Cl	0.45	0.51
Ca	0.30	0.20
Mg	0.26	0.20
Ti	0.08	0.02
P	0.03	0.51
Mn	0.03	0.02
Fe	0.02	0.02
Ba	0.01	0.01
Rb	0.01	0.01

dotted-dotted line represents the hypothetical spectrum of granite with Au at the surface (0.01 in atomic %) but also with Au diffusing in granite (0.005% atomic). Au diffusion is revealed by a clear decreasing tail pointing towards lower energies caused by the energy loss through the sample (Chu et al., 1978). The signal of Au diffusion within the granite can affect the RBS signal of other elements (see for example the variation of K signal) as a result of signal superposition, but no variation of the granite substrate composition is needed to simulate these effects. The spectrum is simulated considering a gold impurity diffusing within the granite substrate.

In RBS analysis, the energy scale is converted to a distance scale (x, diffusion length) given the energy loss in the sample, considering a mean density for the material (ρ), of 2.67 g/cm^3 for granite. The uncertainties related to this assumption of average granite were considered overestimating the uncertainties in the diffusion coefficients calculations.

3.2. Colloid diffusion: RBS results

Fig. 2 shows the RBS spectra of granite after immersion in gold colloid suspensions. Only the spectra in those energies near the region of interest for Au

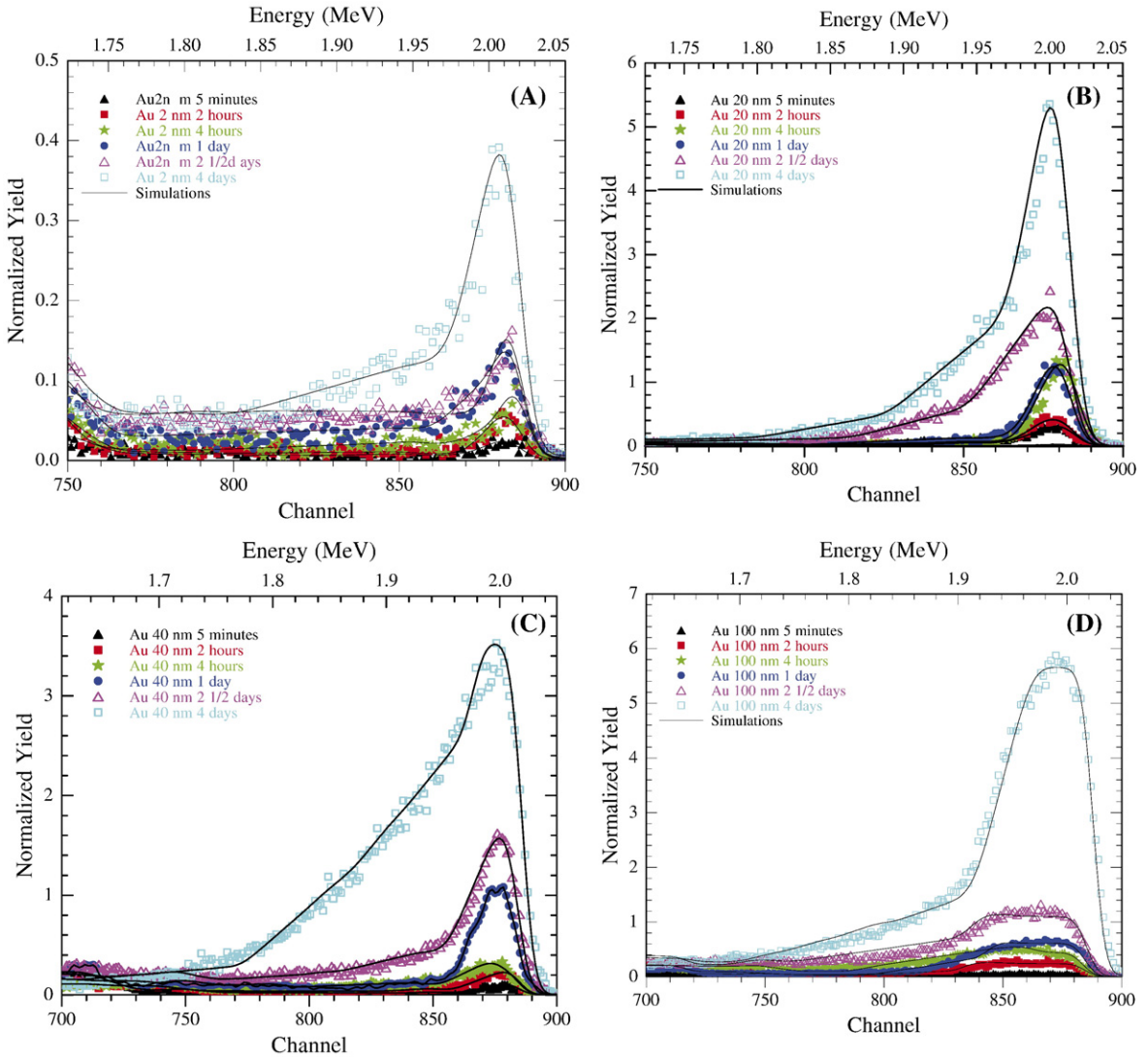

Fig. 2. RBS spectra of granite after the contact with the gold colloids of (A) 2 nm, (B) 20 nm, (C) 40 nm and (D) 100 nm. Contact time: (▲) 5 min, (■) 2 h, (★) 4 h, (●) 1 day, (△) 2 and 1/2 days, (□) 4 days. The simulations are plotted as continuous lines.

(1.85–2.05 MeV) are shown. Fig. 2A, B, C and D present the results obtained with gold colloids of 2, 20, 40 and 100 nm, respectively. For all the RBS spectra obtained, the signal of Au is clearly visible with Au peak height increasing over time, corresponding to an increasing concentration of Au at the surface caused by sorption/deposition. Moreover, the peaks are asymmetrical presenting a tail pointing towards lower energies and are more pronounced over longer times.

Both the existence of the tail of the Au peak pointing towards lower energies and the tail increasing over time, suggested that Au is penetrating in the granite over time, and was therefore diffusing. The RBS spectra of granite in contact with the 250 nm colloids are presented in Fig. 3. The Au is again detected at the granite surface, and the gold peak is quite wide, as expected, resulting from their larger size. However, there is no temporal dependence on the height and tail of the Au peak: therefore the hypothesis that a diffusion process is occurring is difficult to defend.

As explained earlier in this paper, the RBS diffusion profiles of Au were analyzed with the X-RUMP code to determine the diffusion lengths of the Au.

Since the diffusion of colloids and not solutes was studied, the RBS analyses entailed additional difficulties. The system singularity in which surface roughness, particle accumulation on the surface and colloid diffusion coexist required further checks to isolate the different contributions. Both the granite surface morphology and colloid geometry, accounting for different colloid sizes, were considered to distinguish real colloid concentration profiles from other artifacts.

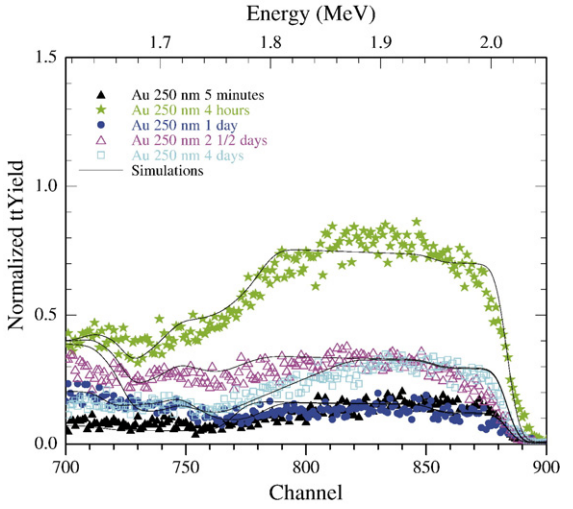

Fig. 3. RBS spectra of granite after the contact with the gold colloids of 250 nm. Contact time: (▲) 5 min, (★) 4 h, (●) 1 day, (△) 2 and 1/2 days, (□) 4 days. The simulations are plotted as continuous lines.

Several authors studied surface topography effects on the features of RBS spectra, as island growth on a surface (Campisano et al., 1975; Slotte et al., 2000; Metzner et al., 1998; Shorin and Sosnin, 1992) or different sample inhomogeneities (Baglin et al., 1998), as spherical or columnar inclusions in a matrix (Stoquert and Szörényi, 2002). In our case, the coexistence of roughness and colloids depth profiles, leads to the overlap of two effects in the Au signal in the RBS spectrum. According to Mayer's model (Mayer, 2002) it is possible to distinguish and theoretically describe two different cases: smooth film on rough surface and rough film on smooth surface.

To evaluate the impact of surface roughness in the diffusion RBS spectra, a separated study was performed (Patelli et al., 2006). A code based on Monte Carlo theory (MC) was developed to define RBS spectra of a smooth film of Au colloids on a rough granite surface. The sample roughness, measured experimentally by AFM, was described by a Lorentzian distribution. The model and complementary measurements demonstrated that samples roughness had no effects on the RBS spectra of diffused Au. In the complementary work (Patelli et al., 2006) it was also demonstrated that the asymmetric measured gold peaks (Fig. 2) and the observed time and size dependence (for colloids from 2–100 nm) can be only reproduced considering that the higher energy contribution of the Au signal came from sphere colloids attached to the surface while the tail of the Au signals came from Au concentration gradient deeper in the granite (Patelli et al., 2006).

3.3. RBS spectra analyses and diffusion coefficient calculations

To demonstrate the occurrence of Au diffusion in granite, the RBS spectra must be simulated either with an equation assuming an Au concentration gradient in the granite and/or analyzing the temporal dependence of diffusion lengths.

To simulate the full spectra with the RUMP code in the same way, an average granite composition, presented in Table 2, was used as "substrate" allowing small variations (<5%) of the Fe or K content. In this "substrate", a Au concentration gradient was introduced to simulate colloid diffusion. A constant Au concentration in the upper layer, with a thickness approximately coincident to one or two layers of the colloid particle size was needed, to account for the presence of colloids

adsorbed/deposited on the surface. These first layers were not considered for estimating diffusion lengths.

In most of the RBS spectra obtained with the 250 nm colloids (Fig. 3), it was not necessary to introduce an Au concentration gradient, since the spectra could be simulated accounting only for a surface signal. Again, it is difficult to defend that diffusion occurs when using 250 nm colloids.

All the simulations, matching the experimental data, are shown as continuous lines in both Figs. 2 and 3. The diffusion lengths were obtained from the Au concentration gradients that more closely match the RBS spectra.

Fig. 4 shows the diffusion lengths, as a function of time, for all sized colloid. Diffusion length increases over time with the smaller colloids presenting larger diffusion lengths, indicating size dependence. Since a clear diffusion process was not observed in the case of 250 nm colloids, they were not included in the plot.

As a first approximation to obtain the diffusion coefficients (D), the dependence of diffusion lengths (x) on time (t) was analyzed. Diffusion length dependence over time in a diffusion-controlled process can be approximated with the equation:

$$x = \sqrt{(Dt)} \tag{2}$$

The experimental data in Fig. 4 were matched using Eq. (2) and the obtained diffusion coefficients are shown in Table 3 including the simulation correlation coefficient (R). Less diffusion is observed with greater colloid size but the maximum variation is limited to one order of magnitude. The minimum and maximum D obtained,

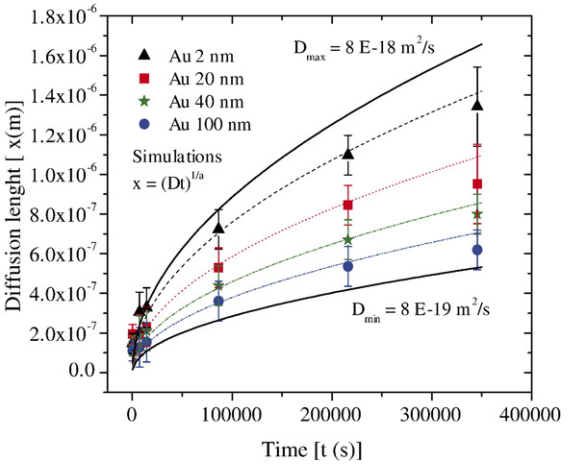

Fig. 4. Diffusion lengths (in m) as a function of the contact time (in s). Colloid size: (▲) 2 nm, (■) 20 nm, (★) 40 nm, (●) 100 nm. The dash lines correspond to the simulation performed with equation (Eq. (2)).

Table 3
Estimation of (apparent) diffusion coefficients as a function of the colloid size, determined by two different methods (with Eqs. (2) and (3))

Colloid size (nm)	D (from Eq. (2)) (m^2/s)	D (from Eq. (3)) (m^2/s) ($t \leq 2$ 1/2 days)	D (from Eq. (3)) (m^2/s) ($t=4$ days)
2	(5.6±0.5) E-18 ($R=0.98$)	(7.0±0.5)·E-18	(3.0±0.5)·E-18
20	(3.4±0.5) E-18 ($R=0.94$)	(3.0±0.5) E-18	(1.0±0.5) E-18
40	(2.1±0.5) E-18 ($R=0.95$)	(2.5±0.5) E-18	(7.0±0.5) E-19
100	(1.4±0.5) E-18 ($R=0.95$)	(1.5±0.5) E-18	(3±0.5) E-19
250	Not determined	Not determined	Not determined

The third column includes the lower D_a required to simulate spectra at 4 days with Eq. (3).

considering possible experimental errors are included in Fig. 4.

In a second step, to strengthen interpretation of the data, direct analysis was performed on the Au concentration profiles within the granite with a RUMP modeling subroutine. From the experimental conditions, the granite can be considered as a semi-infinite medium ($x>0$) where the boundary is maintained at a constant concentration (C_B). The initial concentration is zero throughout the medium.

The equation used to simulate the concentration profiles within the solid was a solution of Fick's second law which satisfies the boundary conditions $C=C_B$, $x=0$, $t>0$ and the initial conditions $C=0$, $x>0$, $t=0$ is (Crank, 1956):

$$C = C_B \mathrm{erfc} \frac{x}{2\sqrt{(Dt)}} \tag{3}$$

Since the determination of the diffusion coefficient is made in transient conditions by analyzing Au concentrations in the solid (where retention may occur) the value is defined as the "apparent" diffusion coefficient (D_a) (García_Gutiérrez et al., 2006).

The D_a values used for simulating the spectra with Eq. (3) are included in Table 3. The determinations were made with a trial and error procedure to obtain the D_a value that best reproduced all the spectra obtained at different times and for each size colloid.

Fig. 5 shows the comparison between the simulation obtained for $t=2$ 1/2 days for the colloids from 2 to 100 nm, using the diffusion coefficient obtained using Eq. (2) (diffusion lengths) or Eq. (3) (erfc function), respectively. For all the spectra collected over shorter times (generally ≤ 2 1/2 days), these coefficients did not

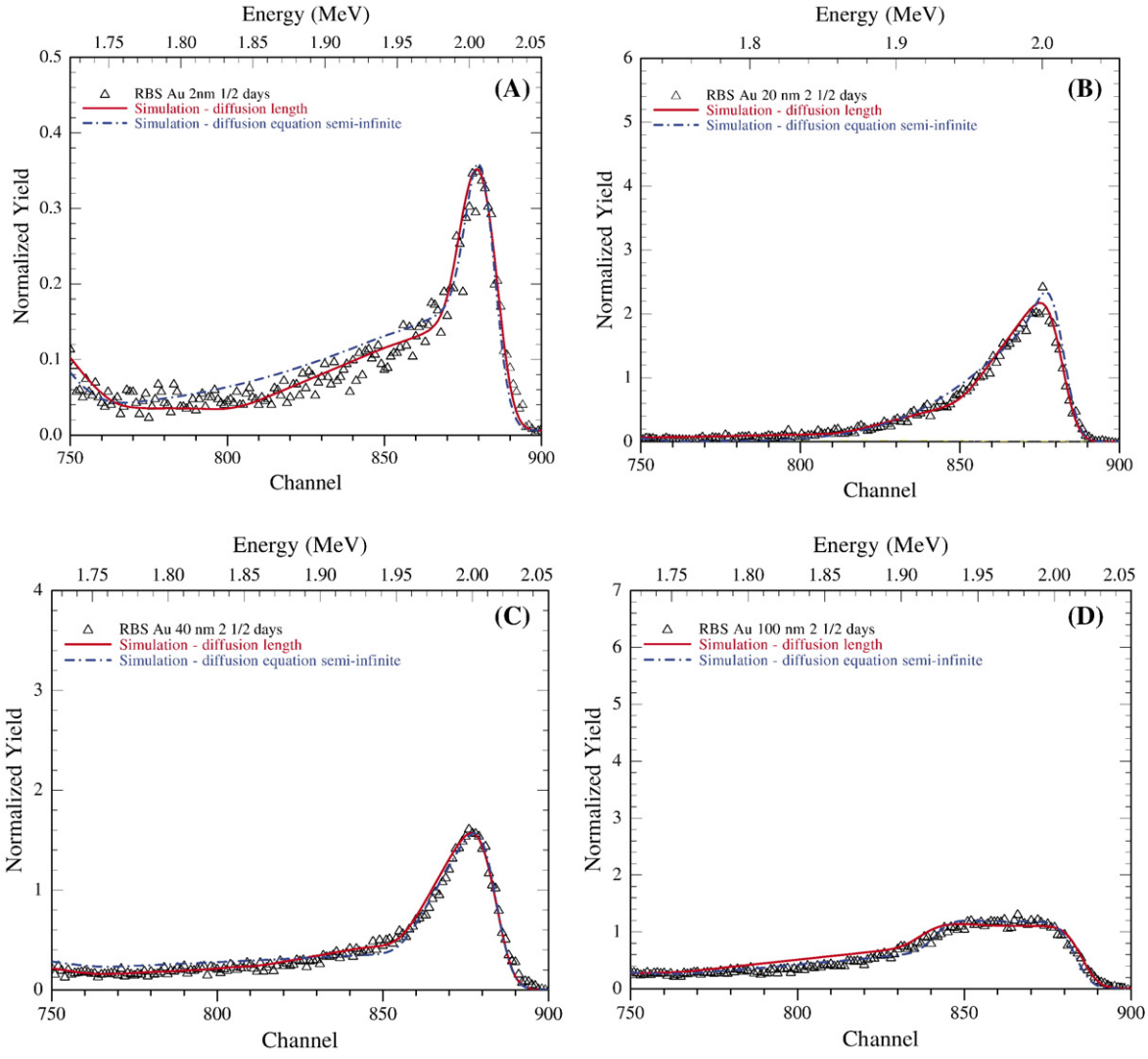

Fig. 5. Comparison of the simulations performed for the RBS spectra using the diffusion coefficients obtained with equation Eq. (2) (diffusion lengths, continuous line) or Eq. (3) (erfc function, dashed-dotted line). (△) RBS spectra of granite samples after the contact with gold colloids suspensions of (A) 2 nm, (B) 20 nm, (C) 40 nm and (D) 100 nm, respectively.

differ significantly from those obtained with the previous method (Eq. (2)) and the simulations of the spectra given these profiles closely matched those presented in Fig. 2. At 4 days Au concentration profiles could not be simulated with Eq. (3) using the same D_a and required a lower diffusion coefficient, a possible indication that, at longer times, particles begin clogging pores, making diffusion more difficult. These values are included in Table 3.

The spectra obtained from the experiment with 250 nm colloids, were simulated with only a gold layer on the surface. When a small concentration gradient was observed it could not be successfully simulated with Eq. (3).

Our results demonstrate that gold colloids, from 2 to 100 nm, diffuse in granite and that, the D_a are all in the range of E-18 m^2/s. These values are about five orders of magnitude lower than a low sorbing solute (U) determined under the same experimental conditions (Alonso et al., 2003a,b). Even when size dependence is observed, it is not pronounced. Oswald and Ibaraki found that matrix diffusion did not increase linearly as colloid size decreased, even if the smallest colloids diffused deeper in the matrix (Oswald and Ibaraki, 2001).

Since this is the first time that the effect of colloid diffusion in granite is experimentally analyzed, the comparison of our data can only be made with

theoretical values. In general, in the literature "effective" diffusion coefficients (D_e) are reported (Ohlsonn and Neretnieks, 1997; García_Gutiérrez et al., 2006).

A short description of the relationship between diffusion parameters is given below. More details on the theory of diffusion in crystalline rock can be found elsewhere (Ohlsson and Neretnieks, 1995; Neretnieks, 1980).

The diffusion coefficient of a spherical particle in an unconfined liquid (D_o), is related to temperature (T), with the dynamic viscosity (η) of the liquid and with the hydrodynamic radius of the particle (r) determined by the Stokes–Einstein equation:

$$D_o = \frac{kT}{6\pi\eta r} \tag{4}$$

where k is the Boltzmann constant. The D_o values calculated for the colloids used in this study, considering a water dynamic viscosity of η=8.9E-4 Pa·s, T=298 K, and the colloid hydrodynamic radius measured by PCS, are included in Table 4. The maximum variation of D_o as a function of colloid size is within 2 orders of magnitude.

In porous media, diffusion occurs in the water within the pores, with tortuosity (τ) and constrictivity (δ) hindering diffusion in solids (Buil, 2002). The diffusivity in the solid pores (D_p) is expressed as:

$$D_p = D_o \frac{\delta}{\tau^2} \tag{5}$$

These D_p values are smaller than the diffusion coefficients in a unconfined liquid (D_o), since the ratio $\frac{\delta}{\tau^2} = G$ (or geometric factor) is less than one. An empirical relationship between G and the accessible porosity (ε) in crystalline rocks is $G = 0.71\varepsilon^{0.58}$ (Parkhomenko, 1967; Jakob, 2004). As mentioned in the Materials and methods section, the measured average porosity of our samples was 0.3%, but for negatively charged species, an accessible porosity one order of magnitude lower than that measured is usually taken (Ohlsonn and Neretnieks, 1997), since colloids suffer anionic exclusion because both the colloids and the granite surface on average are negatively charged. For calculations, an accessible porosity value of 0.03% was considered.

The effective diffusion coefficient (D_e) is related to the pore diffusion coefficient (D_p) by:

$$D_e = \varepsilon D_p \tag{6}$$

The relation between D_a and D_e is given by (García_Gutiérrez et al., 2006):

$$D_a = D_e/\alpha \tag{7}$$

where $\alpha = \varepsilon + \rho \cdot R_d$ is the dimensionless rock capacity factor, and R_d the distribution coefficient.

Table 4 summarizes the apparent diffusion coefficients experimentally found for the different colloids in this study (D_a) and the calculated D_o and D_p values, respectively with Eqs. (4) and (5).

Given the properties of the rock matrix, the D_e for negatively charged Au colloids, calculated with Eq. (6) (ε=0.0003) and included in Table 4, varied from 1.75E-16 m^2/s (2 nm) to 4.3E-18 m^2/s (250 nm). The rock capacity factor and the R_d values were estimated using the experimentally evaluated D_a values with Eq. (7) (also included in Table 4). The R_d values obtained from these analyses, decreased with increasing colloid size from 2.5 ml/g (100 nm) to 9.3 ml/g (2 nm). Small but not null sorption on granite is shown. Smaller particles are more likely to come into contact with the rock surface (James and Chrysikopoulos, 1999; Oswald and Ibaraki, 2001) (because of their higher D_o) explaining their higher probability to attach/sorb to the surface producing higher R_d values. Smaller colloids with higher retention on the rock surface and higher diffusion coefficients will be more easily removed from the flow paths than larger ones.

Table 4
Evaluation of D_o, D_p, D_e, α and R_d for the gold colloids of different size

Hydrodynamicradius (m)	D_a (m^2/s)	D_0 (m^2/s)	D_p (m^2/s)	D_e (m^2/s)	α	R_d (ml/g)
2.70E-09	7.0E-18	9.08E-11	5.83E-13	1.75E-16	25.0	9.37
1.00E-08	3.0E-18	2.45E-11	1.58E-13	4.73E-17	15.8	5.90
2.36E-08	2.5E-18	1.04E-11	6.68E-14	2.00E-17	8.0	3.00
4.75E-08	1.5E-18	5.16E-12	3.32E-14	9.95E-18	6.6	2.48
1.10E-07	ND	2.23E-12	1.43E-14 ε=0.0003 G=6.4E-03	4.30E-18	ND	ND

ND=not determined.
D_a values are the ones experimentally determined from diffusion studies (Table 2).

This study allowed experimentally determining very low diffusion coefficient for colloids (E-18 m^2/s). These diffusion coefficients would not explain alone the tailing behavior of colloid breakthrough curves obtained from colloid transport experiments (James and Chrysikopoulos, 1999; Kosakowsky, 2004; Möri et al., 2003a) if diffusion was the only mechanism accounted for colloid filtration, indicating that matrix diffusion cannot be the only mechanism responsible for colloid filtration.

4. Conclusions

A new methodology based on the RBS technique allowed the evaluation of apparent colloid diffusion coefficients within granite, overturning the belief that colloids did not diffuse within low porosity media.

Apparent colloid diffusion coefficients (D_a) were determined as a function of colloid size, with values from 7E-18 m^2/s for the 2 nm colloids to 1.5E-18 m^2/s for 100 nm colloids. The 250 nm colloids did not diffuse within the rock, emphasizing the influence of the pore to colloid size ratio. Given the properties of granite, the effective diffusion coefficients (D_e) could be estimated, and were several orders of magnitude lower than that of a solute (ranging from 1.75E-16 m^2/s for 2 nm colloids to 4.3E-18 m^2/s for the 250 nm colloids). These diffusion coefficients can be included in models used for evaluating colloid-mediated radionuclide transport in granite. But, these values indicate that, even though matrix diffusion is a possible mechanism, it cannot be the only mechanism responsible for colloid filtration, and thus other filtration mechanisms should be experimentally studied.

Our proposed technique and methodology are applicable to study colloid diffusion within other natural media.

Acknowledgments

The EU is thanked for the support within the FUNMIG project (Ref. FP6-516514) and the EURONS program (FP6 Contract n. 506065), to perform, the RBS measurements at the INFN-LNL (Italy). The Spanish Ministry MEC is thanked for the granted PROMICOL (CGL 2005-01482/BTE) project. The authors thank David R. Peck for English syntactical and grammatical consultations.

Appendix A. Supplementary data

Supplementary data associated with this article can be found, in the online version, at doi:10.1016/j.epsl.2007.04.042.

References

Alonso, U., Missana, T., Patelli, A., Rigato, V., Rivas, P., 2003a. Study of the contaminant transport into granite micro-fractures using nuclear ion beam techniques. J. Contam. Hydrol. 61 (1–4), 95–105.

Alonso, U., Missana, T., Patelli, A., Rigato, V., Ravagnan, J., 2003b. RBS and mPIXE analysis of uranium diffusion from the bentonite to the rock matrix in a deep geological waste disposal. Nucl. Instrum. Methods Phys. Res., B 207 (2), 195–204.

Alonso, U., Missana, T., Patelli, A., Ravagnan, J., Rigato, V., 2004. Experimental study of colloid interactions with rock surfaces. Scientific Basis For Nuclear Waste Management XXVIII. MRS Symposium Procedures 824, Material Research Society, San Francisco, USA.

Alonso, U., Missana, T., Patelli, A., Rigato, V., 2005. Colloid diffusion experiments through granite: size dependence and clogging effects. CIEMAT Technical Report CIEMAT/DMA/M2132/5/05, Madrid, SPAIN.

Alonso, U., Missana, T., Geckeis, H., García-Gutiérrez, M., Turrero, M.J., Möri, R., Schäfer, T., Patelli, A., Rigato, V., 2006. Role of inorganic colloids generated in a high-level deep geological repository in the migration of radionuclides: open questions. J. Iberian Geol. 32 (1), 79–94.

Baglin, J.E.E., Tabacniks, M.H., Kellock, A.J., 1998. RBS as a tool for topographic modelling of polycrystalline thin film interactions, Nucl. Instrum. Methods Phys., Res. B, 136–138, 241–246.

Buil, B., 2002. Caracterización petrológica, mineralógica, geoquímica y evaluación del comportamiento geoquímico de las REE en la fase sólida (granitoides y rellenos fisurales) del sistema de interacción agua-roca del entorno de la Mina Ratones. ENRESA Technical Publication PT-07-02, Madrid, Spain.

Campisano, S.U., Foti, G., Grasso, F., Rimini, E., 1975. Determination of concentration profile in thin metallic-films—applications and limitations of He+ backscattering. Thin Solid Films 25 (2), 431–440.

Chu, W.-K., Mayer, J.W., Nicolet, M.-A., 1978. Backscattering Spectrometry. Academic Press.

Crank, J., 1956. The Mathematics of Diffusion. Claredon Press, Oxford.

Cumbie, D.H., McKay, L.D., 1999. Influence of diameter on particle transport in a fractured shale saprolite. J. Contam. Hydrol. 37, 139–157.

Degueldre, C., Grauer, R., Laube, A., Oess, A., Silby, H., 1996. Colloid properties in granitic groundwater systems. II: Stability and transport study. Appl. Geochem. 11, 697–710.

Doolittle, L.R., 1986. A semiautomatic algorithm for Rutherford backscattering analysis. Nucl. Instrum. Methods Phys. Res., B 15, 227–231.

García-Gutiérrez, M., Cormenzana, J.L., Missana, T., Mingarro, M., Molinero, J., 2006. Overview of laboratory methods employed for obtaining diffusion coefficients in FEBEX compacted bentonite. J. Iberian Geol. 32, 37–55.

Grindrod, P., 1993. The impact of colloids on the migration and dispersal of radionuclides within fractured rock. J. Contam. Hydrol. 13, 167–181.

Hayat, M.A., 1989. In: Press, A. (Ed.), Colloidal Gold, Principle, Methods and Applications, pp. 13–31.

Hellmuth, K.-H., Siitari-Kauppi, M., Lindberg, A., 1993. Study of porosity and migration pathways in crystalline rock by impregnation with 14C-polymethylmethacrylate. J. Contam. Hydrol. 13, 403–418.

http://www.genplot.com/.
Hunter, R.J., 1986. Foundations of Colloid Science I. Clarendon Press, Oxford.
Jakob, A., 2004. Matrix diffusion for performance assessment—experimental evidence, modeling, assumptions and open questions. PSi Technical Report, Villigen, Switzerland.
James, S.C., Chrysikopoulos, C.V., 1999. Transport of polydispersed colloid suspensions in a single fracture. Water Resour. Res. 35 (3), 707–718.
Kelokaski, M., Siitari-Kauppi, M., Sardini, P., Möri, A., Hellmuth, K.-H., 2006. Characterisation of pore space geometry by 14C-PMMA impregnation—development work for in-situ studies. J. Geochem. Explor. 90, 45–52.
Kersting, A.B., Efurt, D.W., Finnegan, D.L., Rokop, D.J., Smith, D.K., Thompson, J.L., 1999. Migration of plutonium in groundwater at the Nevada Test Site. Nature 397, 56–59.
Kosakowsky, G., 2004. Anomalous transport of colloids and solutes in a shear zone. J. Contam. Hydrol. 72 (1–4), 23–46.
Leskinen, A., Penttinen, L., Siitari-Kauppi, M., Alonso, U., García-Gutiérrez, M., Missana, T., Patelli, A., 2007. Determination of granites' mineral specific porosities by PMMA method and FESEM/EDAX. In Scientific Basis for Nuclear Waste Management XXX, edited by D.S. Dunn, C. Poinssot, B. Beg. Mater. Res. Soc. Symp. Proc. 985, 0985-NN11-20,Warrendale, PA.
Mayer, M., 2002. Ion beam analysis of rough thin films. Nucl. Instrum. Methods Phys. Res., B 194, 177–186.
McCarthy, J.F., Degueldre, C., 1993. Sampling and characterization of groundwater colloids for studying their role in the subsurface transport of contaminants. In: Buffle, J., van Leeuwen, H. (Eds.), Environmental Particles, vol. II. Lewis Publishers, Chelsea, MI, pp. 247–315.
McCarthy, J.F., Zachara, J.M., 1989. Subsurface transport of contaminants. Environ. Sci. Technol. 23, 496–502.
Metzner, H., Hahn, T., Gossla, M., Conrad, J., Bremer, J.-H., 1998. Rutherford backscattering spectroscopy of rough films: experimental aspects. Nucl. Instrum. Methods Phys., Res. B 134, 249–261.
Missana, T., García-Gutiérrez, M., Alonso, U., 2006. On radionuclide retention mechanisms in fractured geologic media. J. Iberian Geol. 32 (1), 55–77.
Möri, A., Alexander, W.R., Geckeis, H., Hauser, W., Schäfer, T., Eikenberg, J., Fierz, T., Degueldre, C., Missana, T., 2003a. The colloid and radionuclide retardation experiment at the Grimsel Test Site: influence of bentonite colloids on radionuclide migration in fractured rock. Colloids Surf., A 217, 33–47.
Möri, A., Mazurek, M., Adler, M., Schild, M., Siegesmund, S., Vollbrecht, A., Ota, K., Ando, T., Alexander, W.R., Smith, P.A., Haag, P., Buler, C., 2003b. The Nagra-JNC in-situ study of safety relevant radionuclide retardation in crystalline rock: IV: The in situ study of matrix porosity in the vicinity of a water conducting fracture. NAGRA, Technical Report 00-08, Switzerland, NAGRA, Switzerland.
Neretnieks, I., 1980. Diffusion in the rock matrix: an important factor in radionuclide retardation? J. Geophys. Res. 85 (B8), 4379–4397.
Ohlsonn, Y., Neretnieks, I., 1997. Diffusion data in granite: recommended values. SKB Technical Report TR-97-20, SKB, Stockholm, Sweden.
Ohlsson, Y., Neretnieks, I., 1995. Literature survey of matrix diffusion theory and of experiments and data including natural analogues. SKB technical Report 95-12, Stockholm, Sweden.
Oswald, J.G., Ibaraki, M., 2001. Migration of colloids in discretely fractured porous media: effect of colloidal matrix diffusion. J. Contam. Hydrol. 52, 213–244.
Parkhomenko, E.I., 1967. Electrical Properties of the Rocks, Translated and Edited by George V. Keller. Plenum Press, New York.
Patelli, A., Alonso, U., Rigato, V., Missana, T., Restello, S., 2006. Validation of the RBS analysis of colloid migration through a rough granite surface. Nucl. Instrum. Methods Phys. Res., B 249, 575–578.
Ryan, J.N., Elimelech, M., 1996. Review: colloid mobilization and transport in groundwater. Colloids Surf., A 107, 1–56.
Shorin, V.S., Sosnin, A.N., 1992. RBS spectra for thin films with surface roughness. Nucl. Instrum. Method Phys. Res., B 72, 452–456.
Slotte, J., Laakso, A., Ahlgren, T., Rauhala, E., Salonen, R., Simon, A., Uzonyi, I., Kiss, A.Z., Somorjai, E., 2000. Influence of surface topography on depth profiles obtained by Rutherford backscattering spectrometry. Journal of Applied Physics 87 (N.1), 140–143.
Smith, P.A., Degueldre, C., 1993. Colloid-facilitated transport of radionuclides through fractured media. J. Contam. Hydrol. 13, 143–166.
Stoquert, J.P., Szörényi, T., 2002. Determination of the number and size of inhomogeneities in thin films by ion beam analysis. Phys. Rev., B 66 (14), 144108.